EPJ Web of Conferences **343**, 02003 (2025) https://doi.org/10.1051/epjconf/202534302003
AIMACE-2025

Investigation of variation in the leading edge shapes on the aerodynamic characteristics over a delta wing

Sugandh Gupta*[1], *Rakesh* Kumar[2], *Sanjeev* Kumar[3], Tushar Siag[4]
[1]Department of Aerospace Engineering, Chandigarh University, Punjab, India
[2]Department of Aerospace Engineering, Punjab Engineering College, Chandigarh, India
[3]Department of Mechanical Engineering, Punjab Engineering College, Chandigarh, India
[4]Florida State University, USA

Abstract. The present study deals with the effect of varying the slender delta wing's leading edge shapes on the aerodynamic characteristics using a subsonic wind tunnel. A force balance system computed the surface pressure measurement for three leading-edge shapes. The leading edges for the present study are sharp, circular and hybrid. The angle of attack is varied from 0o to 35o and has a freestream velocity of 15m/s. The lift and drag coefficients were computed and compared for all the leading edge shapes of the delta wing. The comparative analysis depicts the highest aerodynamic efficiency for the delta wing with a circular leading edge. Based on the results obtained from the surface pressure distribution, the circular leading edge possesses the highest vortex strength and further delays the flow separation, thereby increasing the operating range of the angle of attack.

Keywords: Wind Tunnel Testing, Leading-edge, Aerodynamic characteristics, 65-degree Delta wing, Coefficient of Pressure (C_p), Leading Edge Vortices (LEV)

1 Introduction

Delta wings are triangle-shaped wings used mostly for high-speed applications in aircraft and missiles. Delta wings have become increasingly popular in the aerospace industry due to their superior aerodynamic performance, particularly at high speeds and low altitudes. The reason for using delta wings in supersonic flight is their ability to reduce supersonic wave drag, thereby improving cruise performance. The primary users of this technology are the armed forces throughout the world. As the militaries around the world need to react quickly to a potential threat, hence, delta wings' find their application in supersonic fighter aircraft and missiles. Recently, there has been experimentation of this technology in civilian aircraft to provide faster travel around the world. Delta wings have unique aerodynamic characteristics that make them attractive for certain applications, such as high-speed and supersonic aircraft. However, the performance of delta wings can be affected by various factors, including their size, shape, angle of attack, and airspeed. Therefore, research is needed to better understand the behaviour of delta wings in different

* Corresponding author: *sugandh.gupta90@gmail.com

subsonic conditions, and to optimize their design and performance accordingly. Also, constant efforts are being made to utilize delta wings in unmanned aerial vehicles (UAVs), which are becoming increasingly popular in various civilian and military applications. However, UAVs typically operate at lower speeds than supersonic aircraft, and their aerodynamic requirements may differ from those of manned aircraft. Therefore, research on delta wings in the subsonic region can help improve the efficiency and reliability of UAVs, and enhance their ability to perform a wide range of missions. One contemporary issue related to delta wings in the subsonic region is the challenge of maintaining stability and control at low speeds.

The problem with the delta wing is the poor aerodynamic performance of the delta wings at subsonic speeds (M<1). The reason for poor performance is the absence of leading-edge vortices. In a conventional wing, a vortical flow is created around the leading edges of the wing due to pressure difference. These vortices provide an additional vortex lift at a moderate angle of attack which prevents stall [10]. Another problem with delta wings at subsonic speeds is that they can experience flow separation, which can lead to a loss of lift and control authority. Delta wings have a highly swept leading edge, which causes the airflow to deflect and flow along the surface of the wing. The flow separation problem can be particularly acute for unmanned aerial vehicles (UAVs) that need to operate at low speeds for certain missions, such as surveillance and reconnaissance. At low speeds, the flow separation problem can make it difficult to maintain stability and control, which can compromise mission success and safety. These aerodynamic problems collectively limit the applications of delta wings in civilian aircraft, because if applied, they might lead to aircraft crashes during take-off and landing due to stalls caused at low speeds. Most of the research as well is focused on the performance of delta wings at supersonic regimes, which makes it urgent to research the wing in subsonic regions. Overall, the challenges with delta wings at subsonic speeds mentioned above are ongoing and require continued research and development to improve the efficiency and reliability of delta-winged aircraft.

The effects of leading-edge shape and vortex burst on the flow field of a 70-degree-sweep delta wing were investigated [3]. The authors conducted wind tunnel experiments to examine the wing's aerodynamic characteristics, including lift, drag, and vortex shedding, at various angles of attack and with different leading-edge shapes. They found that the shape of the leading-edge strongly influenced the location and strength of the vortex burst and the wing's overall aerodynamic behavior. The study also showed that the vortex shedding frequency was affected by the wing's aspect ratio and sweep angle.

Using a low-speed wind tunnel it was investigated on a half-span delta wing's aerodynamic performance with a leading-edge of 45^0 [8]. The test has been carried out in a subsonic regime under these flow conditions; Mach number of 0.1, 8.37 x 10^5 Reynolds number, AOA ranging from 0^0 - 25^0. Their experimental analysis is based on the pressure modelling of the subsonic wind tunnel, for which pressure tappings have been on the half-span delta wing from root to tip. the results show that the majority of the lift generated by the wing occurs near the L.E. For all angles of attacks, additionally, the lift is generated near the root chord rather than near the tip chord. While drag force increases from the tip to the root, emphasizing the point that Drag forces can reach 60% in the case of 25^0 of the angles of attack.

The researchers created & tested three models, including one with a sharp and two others with circular and semi-circular leading edges of different radii [12]. They found that both the radius of the leading edge along with location and size of vortices were responsible for the moments and forces generated on a 50° delta wing. The study also revealed that the displacement of the vortex burst caused changes in the lift

It was examined that the vortex characteristics of three different delta wing setups [11]: flat, saw-tooth, and sinusoidal tooth. A low-speed wind tunnel is used for experiments including flow measurement at low speeds and oil flow observation at various velocities. The other researchers [10] presented research work based on the surface pressure model for simple delta wings at high angles of attack, which is necessary for predicting aerodynamic loads and stability. To calculate surface pressures on delta wings, the author employs a mathematical approach based on the vortex panel method. The model was validated and compared to other existing models using experimental data. The results show that the proposed model predicts surface pressures and aerodynamic coefficients more accurately than other models.

The investigation on the flow of a 65° delta wing in the Langley National Transonic Facility, NASA was conducted [5]. The study aimed to obtain detailed data on the aerodynamic performance of the delta wing in transonic flow regimes and to investigate the complex flow phenomena that occur in such regimes. The study's findings revealed that the flow characteristics of the delta wing in transonic flow regimes are highly complex and depend on a variety of variables such as air AOA, Mach number, and Reynolds number. The delta wing was discovered to exhibit a variety of complex flow phenomena, such as shock wave and boundary layer interactions, vortex shedding, and vortex breakdown. The authors also saw the formation of a complex flow structure downstream of the delta wing, which included multiple vortices and shock waves. Overall, the authors concluded that the research provides useful information about the aerodynamic performance of delta wings in transonic flow regimes. The study's findings could be useful in the design and optimization of high-speed aircraft operating in such regimes. The study emphasizes the significance of experimental techniques in comprehending the complex flow phenomena observed in high-speed aerodynamics.

An experimental investigation that used an Open Circuit type wind Tunnel equipping Rollab six-component balance for Force/ Moment Modelling. Numerical analysis was performed using GAMBIT and CFD FLUENT [1]. The outcomes of both models were compared. They compared their experimental results to their CFD results, previous research experiment results, and Polhamus theory results [22]. The experimental results for aerodynamics (coefficient of lift and induced drag coefficient) agree well with the CFD results and the Polhamus theory results [22]. Furthermore, the experimental results for the spanwise pressure coefficient agree perfectly with the CFD results. Overall, their experimental results match CFD predictions and theoretical calculations. Furthermore, their results show that, while the Delta wings are designed to perform at supersonic speeds, their (Delta wings) performance is significant even at subsonic speeds (Low-Speed Wind-Tunnel facility).

Computational simulations of 65^0 Delta and $65^0/40^0$ double-delta wings were performed to investigate the effects of primary vortices on aerodynamic properties [2]. They performed the computational simulation on the delta wing of 65^0 sweep and double delta Wing of the

double sweep of $65^0/40^0$ using ICEM-CFD (Integrated Computer Engineering and Manufacturing – Computational Fluid Dynamics software and validated their results by comparing them with the previous experimental literature. Both wing designs are modelled using CATIA software, analyzed using ICEM-CFD software and solved using a CFX solver. The best model suitable for flow variation calculation on and around the wing is the SST Turbulence model hence used over the unstructured mesh. Models have been tested at 13 m/s of velocity for 0^0 to 40^0 of the angles of attacks, maintained temperature is 300^0 K and pressure is 1 atm. Obtained aerodynamics characteristics such as C_L and C_D are calculated and their respective plots versus AOA are generated. Afterwards, the CFD results are compared to the experimental results from the mentioned literature, and with just a 2 percent error, the results show good agreement with the experimental data. Additionally, implementation of a C-section at the leading edge of these wings shows the reduction in vortices formation hence drag and ultimately improves the Lift-to-Drag ratio of these designs.

Wind tunnel testing on various profiles of leading-edge including geometric shapes such as circular, square and other shapes such as beveling, leeward surface beveling, windward surface and wedge, found that windward beveling generated the most organized vortex at the leading-edge and the largest leading-edge flow angle [7]. Additionally, altering the leading-edge profile of the delta wing affected the development of the three-dimensional vortex on the leeward side. The study concluded that the configuration of beveling on a windward surface ensured for formation of a vortex structure at the leading edge at a pitching angle of 10° and emphasized on importance of geometrical shape for the leading-edge profile in preparing a delta wing model for experimentation. Their study found that windward beveling on the leading edge produces the most organized leading-edge vortex and the largest leading-edge flow angle. Varying the leading-edge profile of the delta wing affects the development of the three-dimensional vortex on the leeward side. The configuration of the leading-edge beveling on the windward surface ensures the formation of the leading-edge vortex structure at an angle of attack of 10 degrees. The study highlights the importance of the geometrical shape of the leading-edge profile in preparing a delta wing model for experimentation.

The comparison of the tapered delta wing (Sweep = 50^0) and a modified trailing-edged delta wing (Swift Delta Wing) under similar flow conditions was investigated. An experimental setup has been made underwater to observe the hydrodynamics of both wings at different AOAs and Re numbers. The sectioning of both wings has been made span-wise to visualize and compare the flow at respective sections. Swift causes the breakdown of the vortex, unlike the tapered delta wing under which vortex reattachment is happening due to the chord length of the wing. Also, dual-LEV has been seen over the non-slender tapered Delta wing, however, no such dual vortex has been seen over the swift wing. But suggested comments have been made that if the flow fields reported over swift wings do differ from those of delta wings, it is not due to the tapering of the wing, but to other variables such as wing surface texture or leading-edge geometry.

An analysis of the effects of Reynold's number and leading-edge bluntness on a delta wing with a sweep of 65 degrees was carried out [4]. The Mach number of the freestream was 0.4. The Reynold's number varies from low to high at 6 million and 60 million. The experimental data obtained shows that the flow separation in the blunt-edge case could be

different from the sharp-edge counterpart. The leading-edge pressures were also utilized to find out the origin of the blunt leading-edge vortex separation.

The investigation of the leading-edge flaps on the lift production in a delta wing have been carried out [6]. The testing was done in the subsonic range on delta wings with a sweep of 60 and 75 degrees respectively. After conducting research for various flap deflection angles, it was observed that there was a large increase in the coefficient of lift at low to moderate angles of attack due to the lift generated by a strong vortex. In the end, not only was there an increase in the coefficient of lift, but, the longitudinal stability was maintained as well.

2 Experimental Setup

In this section methodology/ steps followed to carry out the experimental analysis of the delta wings with variation leading edges have been described. Analysis of Features and Finalization Subject to constraints discuss the process of analyzing the design features of the delta wing and finalizing the design subject to various constraints. This section provides a detailed explanation of how the final design of the delta wing was selected, and how it meets the various constraints and design criteria. This will help to ensure that the final design is optimal for the project goals and objectives and that it is practical to manufacture and test.

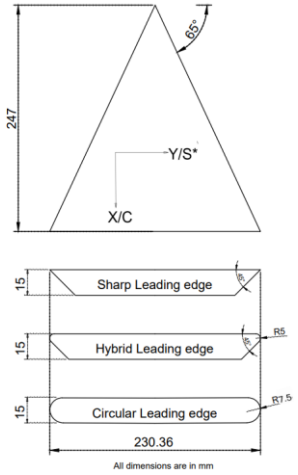

Figure 1 Dimensions of Delta wing (all dimensions in mm)

Table 1 Dimensions of Delta Wing

Model Parameter	**Value**
Root Chord	0.247 m
Sweep Angle	65^0
Bevel Angle	45^0

Span	0.23036 m
Maximum Thickness	0.015 m
Planform Area	0.0284761 m^2
Aspect Ratio	1.86

Table 1 presents the final design of the delta wing, including all relevant specifications and features and the wind tunnel setup. The experimental setup used for the project was a subsonic wind tunnel which was an open circuit and could work for speeds up to 60 m/s. The test section was 600mm x 600mm with a length of 2000 m. The wind tunnel comprises of 8 propeller blades with constant pitch and it is driven by a 3-phase motor. The maximum speed that the motor used in the setup can achieve is 1440 RPM. The temperature at which the wind tunnel had been operated was 27^0 degrees. The wind tunnel is capable of force model testing as well as pressure model testing. Force model testing helps in calculating the aerodynamic forces on a body at given flow conditions. Here, a platform attached at the bottom of the wind tunnel is used which has six degrees of freedom (6-DOF). A suitable stand is provided with a precision 6-component Force Transmitter to mount the Delta wing. A digital Force indicator to measure lift force; drag force; side force, yaw moment and pitching moment is provided. The indicator is calibrated to measure in Newtons (N). The pressure was recorded at various locations on the upper surface of the Delta wing. The displacement in the water level of manometer tubes was noted down and was used further for pressure calculations. This was the manual method of pressure testing, whereas the silicon tubes could also be connected directly to the data acquisition system and the desired values could be obtained directly. The wind tunnel also consisted of a pitot tube which could be mounted inside the test section and was connected to a U-tube differential pressure manometer. Through this differential manometer, the static as well as dynamic pressure could be measured. To adjust the angle of attack of the delta wing model, an adapter was fabricated out of mild steel, which was mounted on the steel rod attached to the motion platform. The model was mounted on the adapter itself. The adapter was rectangular and was made by connecting two U-shaped sections of 102 mm x 102 mm. The adapter could facilitate an angle of attack from 0° to 90°.

The pressure is measured at various locations on the upper surface of the delta wing. In the experimental setup, the Leading edge consists of the following (X/C, Y/S*) locations: (0.2, 0.868), (0.4, 0.868), (0.6, 0.868), (0.8, 0.868). Chord Line consists of the following (X/C, Y/S*) locations: (0.2, 0.0), (0.4, 0.0), (0.6, 0.0), (0.8, 0.0). Intermediate locations between the chord line and the leading edge where pressure is recorded are grouped into two groups for easy analysis: Group 1: (0.4, 0.434), (0.6, 0.289), (0.8, 0.217) Group 2: (0.6, 0.578), (0.8, 0.434) The Variation of Cp along all these locations at all angles of attacks is as follows:

Figure 2 Subsonic Wind Tunnel facility

2.1 Wind Tunnel Testing

Accurate data collection in a wind tunnel is crucial for obtaining meaningful results, hence, some protocols were used for obtaining accurate results, which were as follows:

- Calibration: it was ensured that all the instruments used for measurements such as vernier callipers were calibrated. It was also made sure that the wind tunnel was calibrated so that it did not provide faulty values.
- Stable and uniform flow: Initially when the wind tunnel is started, the flow tends to be irregular which might affect the results. So, the wind tunnel was left turned on for at least five minutes before noting down the readings in order to allow the flow to become stable.
- Minimized interference: It was made sure that no object other than the model itself was there in the wind tunnel to avoid flow interference. For the pressure model, the silicon wires were arranged such that they did not interfere with airflow around the lift-producing surfaces.
- Multiple runs: To ensure that the wind tunnel is providing accurate results, at least three runs were performed on a particular model. It was done to make sure that the wind tunnel was properly calibrated and did not provide faulty readings.
- Proper data acquisition and analysis: To obtain the readings to the maximum decimal points, the data provided by the data acquisition system was stored in an Excel file. The graphs were plotted using Microsoft Excel to avoid any plotting errors caused by plotting manually on graph papers.

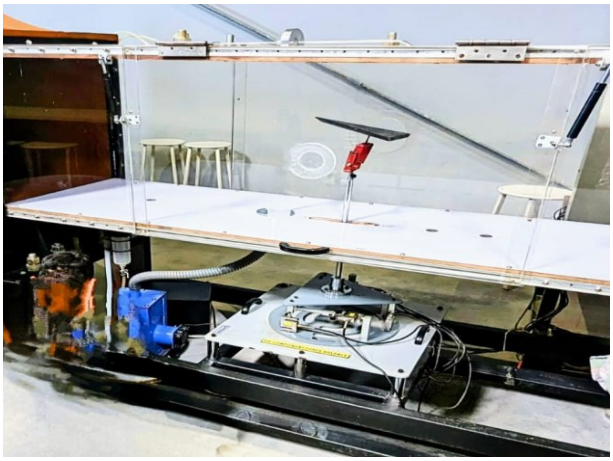

Figure 3 Delta wing model mount for Force Testing in the Wind Tunnel

3 Results and Discussion

3.1 Validation of Experimental Results for Sharp Leading Edge Delta Wing

For validation, the available data was used from the literature [10]. A surface pressure model for simple delta wings at high angles of attack is used for the comparison. This reference paper has been used for the validation of the experimental results obtained through the pressure testing of a delta wing with a sharp leading edge. The values of the Coefficient of Pressure (C_p), along the chord line in this paper were compared with the experimentally obtained values along the chord line. Table 2 shows the experimental pressure distribution along the chord locations for various angles of attack. Table 3 compares the pressure distribution between the experimental and the available results in the literature. The comparison of the results is shown in Figure 4.

Table 2 C_p along the Chord for various AOA's (Experimental)

	C_p along the CHORD				
	X/C	**0.2**	**0.4**	**0.6**	**0.8**
	Y/S*	**0.043**	**0.021**	**0.014**	**0.011**
AOA	0^0	-0.1057679	-0.0705119	-0.070511	-0.21153
	5^0	-0.03526	1.02E-16	-0.07051	-0.21154
	10^0	1.02E-16	1.02E-16	1.02E-16	-0.21154
	15^0	0.141024	0.070512	1.02E-16	-0.21154
	20^0	0.35256	0.211536	0.141024	-0.07051
	25^0	0.35256	0.282048	0.141024	-0.07051

	30^0	0.59935194	0.35255997	0.2820479	1.02E-16
	35^0	0.599352	0.423072	0.423072	0.070512

Table 3 C_p along the Chord for 20^0 AOA (Experimental vs Literature)

C_p at 20^0 AOA Experimental vs Literature [10]		
X/C	20^0 AOA	(Pashilkar, 2001)
0.2	0.35256	0.3
0.4	0.211536	0.26
0.6	0.141024	0.24
0.8	-0.07051	-0.06

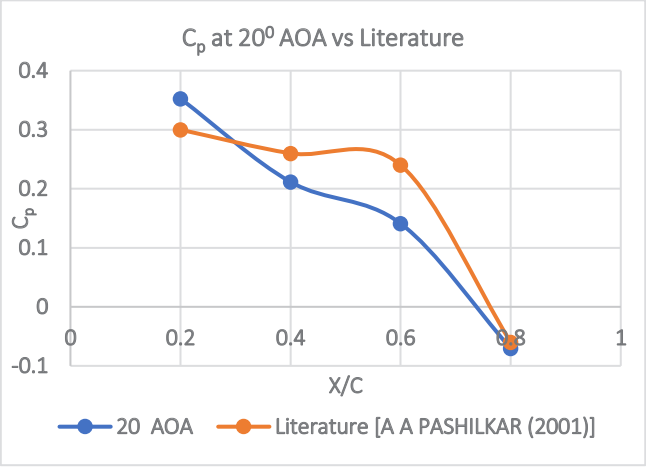

Figure 4 C_p along the Chord for 20^0 AOA (Experimental vs Literature)

Table 4 C_p along the Chord for 35^0 AOA (Experimental vs Literature)

C_p at 35^0 AOA Experimental vs Literature		
X/C	35^0 AOA	(Pashilkar, 2001)
0.2	0.599352	0.59
0.4	0.423072	0.5
0.6	0.423072	0.46
0.8	0.070512	0.07

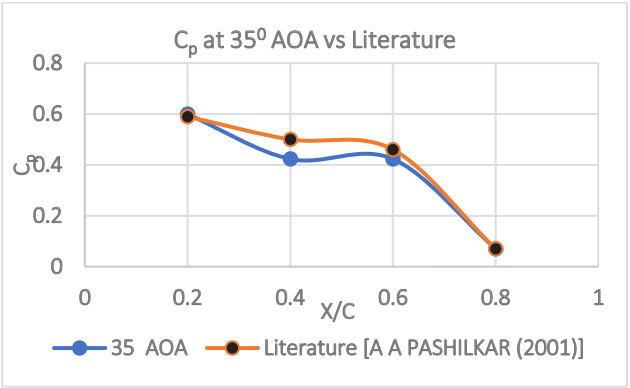

Figure 5 C_p along the chord for 35^0 AoA (experimental vs literature)

From the above data comparison shown in Table 4 and Figure 5, the experimental results are in good agreement with the results available in the literature, which provides proof of accuracy for the results obtained and hence validates the results. The Lift to drag ratio is validated for sharp leading-edge delta wing by comparing the experimental data with the literature [11].

The following were the technical parameters:

- Leading-edge Sweep = 60^0;
- Leading-edge geometry = Sharp, Saw-tooth, Sinusoidal
- Freestream Velocity = 15.37 m/s
- Angle of Attack (α) = 10°, 40°

Table 5 Comparison of L/D for various AOA's (Experimental vs Literature)

AOA	**L/D Experimental**	**L/D Literature [11] (Ramakrishna *et al.*, 2019)**
0^0	4.25	Data not available
5^0	5.75	Data not available
10^0	6.6	6.7
15^0	8	8.36
20^0	10.44444	10.9
25^0	11	11.2
30^0	11.83333	11
35^0	11.06667	10.96

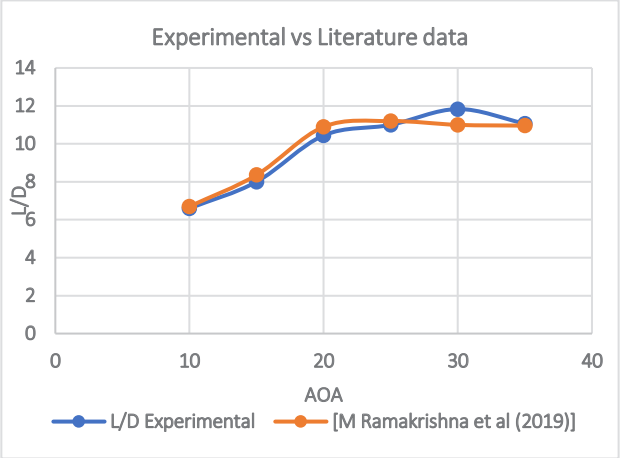

Figure 6 L/D Comparison b/w Experimental and Literature Data

From the data shown in Table 5 and Figure 6, the experimental data is close to Literature [11] which provides proof of accuracy and hence validates the results obtained.

The C_p (pressure coefficient) variation on the surface of a delta wing indicates the distribution of pressure over the wing surface at a particular angle of attack and flight condition. The pressure coefficient is a dimensionless parameter that describes the pressure distribution on a surface, normalized by the free-stream dynamic pressure.

In the case of a delta wing, the C_p variation on the surface can indicate several important features of the flow field, such as the location of the leading-edge vortex, the strength of the vortex, and the presence of shock waves. A positive C_p value indicates that the pressure at that point is higher than the free-stream pressure, which could be an indication of the location of the leading-edge vortex.

- In a delta wing, the leading-edge vortex is formed at the apex of the delta and is responsible for generating lift. When the flow of air over the delta wing separates at the leading edge, it forms a vortex that rolls up and trails behind the wing.
- As the air flows over the delta wing, it experiences a change in direction and encounters regions of compression and expansion. This causes the pressure to vary along the surface of the wing.
- In the region near the leading edge of a delta wing, where the vortex is formed, the air flows downward and inward towards the apex, causing a reduction in pressure. This low-pressure region results in a positive pressure coefficient (C_p) value on the surface of the wing.
- Therefore, a positive C_p value in the region near the leading edge of a delta wing can be an indication of the presence of a leading-edge vortex.

Similarly, a negative C_p value indicates that the pressure at that point is lower than the free-stream pressure, which could be an indication of the presence of a shock wave or a separated flow region.

- In a delta wing, a negative C_p value at a particular point on the surface indicates that the pressure at that point is lower than the free-stream pressure. This pressure

reduction is often associated with flow separation, which occurs when the airflow over the wing separates from the surface and forms a region of recirculating flow.

- When the airflow separates, the boundary layer becomes thicker, and the pressure within it drops. This can cause a decrease in the pressure coefficient, which is a measure of the pressure at a point normalized by the free-stream pressure.
- A delta wing, negative C_p value at a particular point could indicate the presence of a separated flow region. This can occur when the angle of attack is too high or when the flow is too turbulent, causing the airflow to separate from the surface and form a recirculation zone.
- Flow separation can have a significant impact on the aerodynamic performance of a wing, as it can cause a loss of lift and an increase in drag. Therefore, it is important to identify and analyze any areas of flow separation on a delta wing to understand how it affects the wing's overall performance and optimize its design accordingly.

3.1.1 Pressure Coefficient for Sharp Leading-Edge

C_p along the Leading edge from X/C 0.2 to 0.6 is positive which indicates the presence of Leading-edge vortex. This indicates that a vortex is being created and it helps in the generation of lift. There is an increase in the value of Positive C_p from 0° AOA to 30° AOA. The C_p value is higher at one location than others, it could indicate that the vortex is stronger or more concentrated at that location. At X/C 0.8 the C_p value is negative which Indicates the separated flow. Figure 7 indicates the variation of Cp along the leading edge at various locations (X/C) corresponding to the Chord line. Region A indicates the presence of a Leading edge vortex for all angles of attacks. Region B indicates the flow separation at X/C 0.8, i.e. towards the rear of the delta wing.

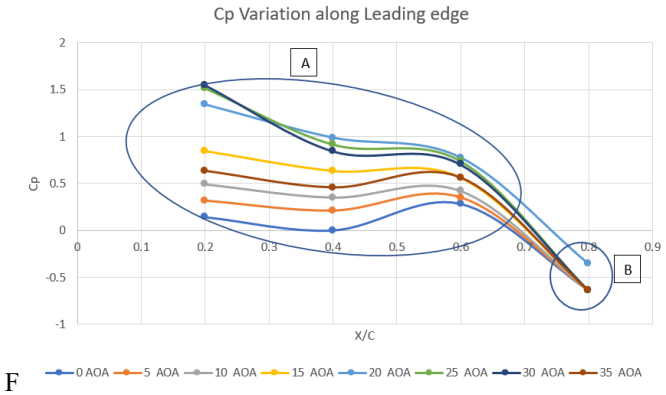

F

Figure 7 C_p Variation along the Leading Edge

Along the chord line, C_p has a higher value at the start of the chord line and the value of C_p is low at the rear end of the wing, which shows a suction region at the rear of the wing. Figure 8 shows that upon comparison among Region A and Region B, the start to the leading edge shows higher C_p than the rear Region B which shows the creation of the suction region that leads to the generation of suction lift.

At Group 1 locations, as shown in Figure 9, C_p grows from negative to positive which indicates that Region A is a Flow separation region and along the wing span, at the rear end

(X/C 0.8) Region B, the C_p is positive for angles of attacks, which indicates the presence of vortex in the region

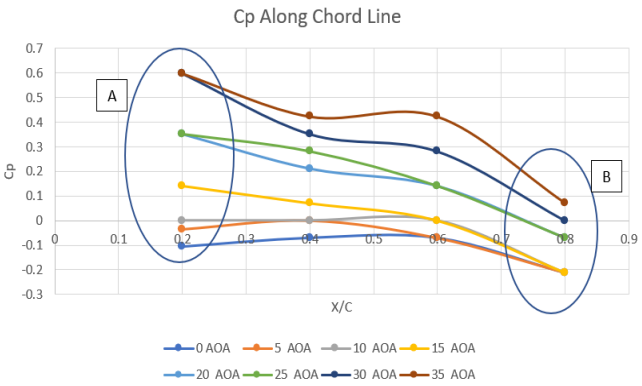

Figure 8 C_p Variation along the Chord Line

At group 2 locations, the C_p value remains positive in both regions A and B which shows the presence of a vortex in the regions, but the slope is negative for the above shown variation. So, the vortex strength decreases with increasing X/C shown in Figure 10.

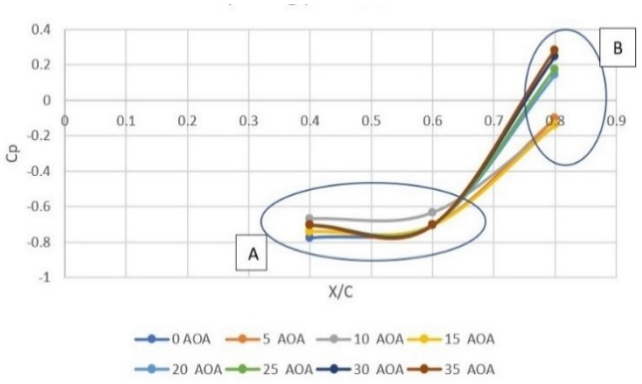

Figure 9 C_p Variation along Group 1

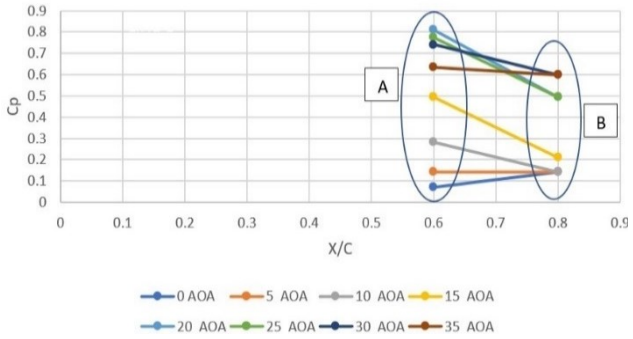

Figure 10 Cp Variation along Group 2

3.1.2 Pressure Coefficient for Circular L.E

The C_p along the Leading edge from X/C 0.2 to 0.6 is positive, which indicates the presence of a Leading-edge vortex. This indicates that a vortex is being created, and it helps in the generation of lift. There is an increase in the value of positive C_p from 0º AOA to 30º AOA. The C_p value is higher at one location than others, it could indicate that the vortex is stronger or more concentrated at that location. At X/C 0.8, the Cp value is negative, which Indicates the separated flow. Figure 11 indicates the variation of C_p along the leading edge at various locations (X/C) corresponding to the chord line. Region A indicates the presence of a Leading edge vortex for all angles of attacks. Region B indicates the flow separation at X/C 0.8, i.e. towards the rear of the delta wing.

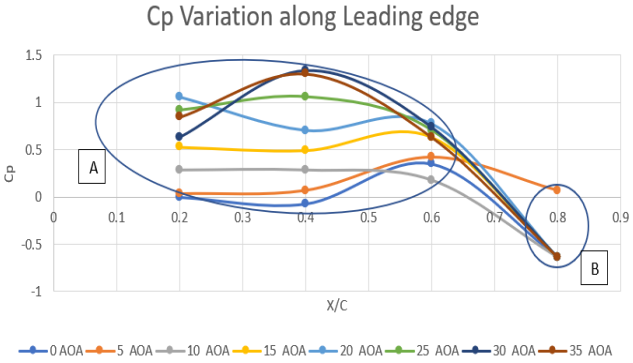

Figure 11 C_p Variation along the Leading Edge

Along the chord Line, it can be seen that the C_p has a higher value at the start of the chord Line and the value of C_p is low (negative) at the rear end of the wing. This shows the strength of the vortex is reducing and a Suction region at the rear of the wing is being created. Figure 12 shows the comparison between Region A and Region B, the Cp at the start of the chord line shows a higher Cp than the rear (Region B) which shows the creation of the suction region that leads to the generation of lift.

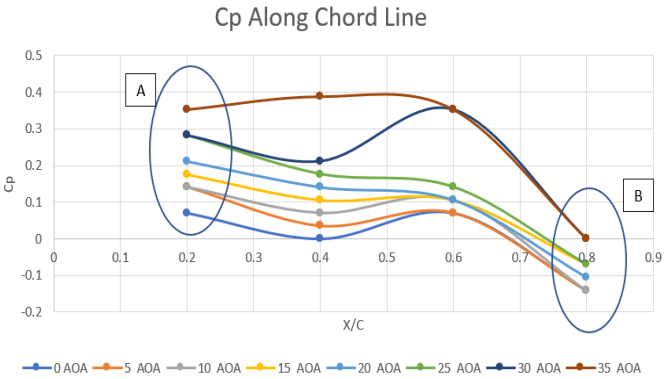

Figure 12 C_p Variation along the Chord Line

At Group 1 locations, shown in Figure 13, C_p grows from negative to positive which indicates that region A is a flow separation region and along the length of the wing, at the rear end (X/C = 0.8) region B, the C_p is positive for some angles of attacks, which indicates the presence of vortex in the region.

At Group 2 locations, shown in Figure 14. The C_p value remains positive in both regions A and B which shows the presence of a vortex in the regions, but the slope is negative for the above shown variation. So, the vortex strength is decreasing with increasing X/C. whereas at AOA 25^0 the slope is positive, which indicates the strength of the vortex increases with the increase in the angles of attack.

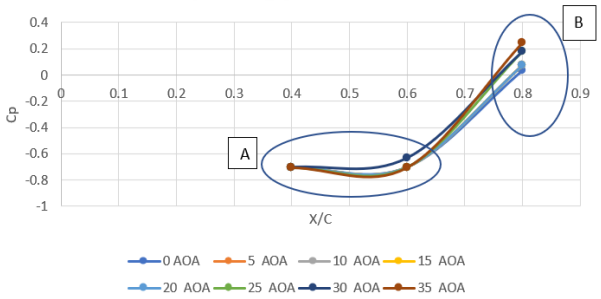

Figure 13 C_p Variation along Group 1

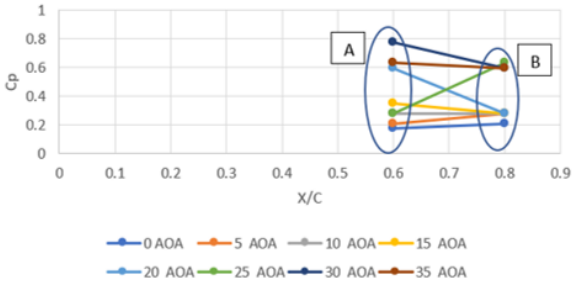

Figure 14 C_p Variation along Group 2

3.1.3 C_p Analysis for Hybrid Leading-Edge

At leading Edge: C_p along the Leading edge from X/C 0.2 to 0.6 is Positive which indicates the presence of a Leading-edge vortex. This indicates that vortex is being created and it helps in the generation of lift. There is an increase in the Value of Positive C_p from 0 AOA to 35 AOA. the Cp value is higher at one location than others, it could indicate that the vortex is stronger or more concentrated at that location. At X/C 0.8 the C_p value is negative which Indicates the separated flow. graph (in Figure 15). indicates the variation of C_p along the leading edge at various locations (X/C) corresponding to the Chord line. Region A indicates the presence of the Leading edge vortex for all angles of attacks Region B indicates the flow separation at X/C 0.8, i.e. towards the rear of the delta wing

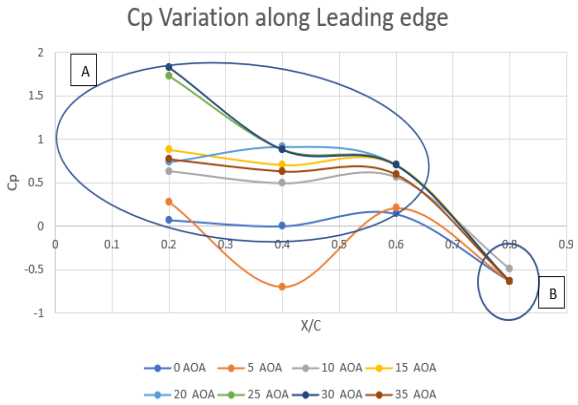

Figure 15 C_p Variation along the Leading Edge

Along the chord line, it can be seen that the C_p has a higher value at the start of the Chord line and the value of C_p is low at the rear end of the wing. At AOA 10, 15 and 25 the C_p is negative at X/C 0.8 which indicates the flow separation region and creation of suction lift. In other cases, the C_p is still positive which shows that the vortex is stretched and is being sustained till the rear end of the wing which is beneficial for the delta wing. Figure 16 shows the comparison between Region A and Region B, the start to the leading-edge shows higher C_p than the rear (Region B) for most of the cases, which shows the creation of a suction region that leads to the generation of lift, whereas at AOA 0°, 5° and 20°, the C_p is positive, but the magnitude is comparatively higher than other AOAs. Which Indicates the better performance of wing at these AOAs

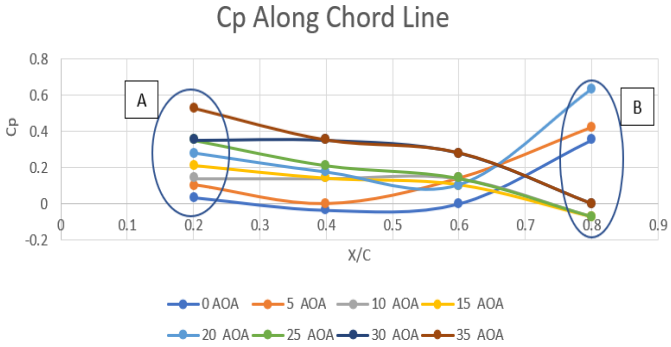

Figure 16 C_p Variation along the Chord Line

At Group 1 locations, shown in Figure 17, Cp grows from negative to positive which indicates that region A is a flow separation region and along the length of the wing, at the rear end (X/C 0.8) region B, the C_p is positive for wide range of angles of attacks except 0°, which indicates the presence of vortex in the region

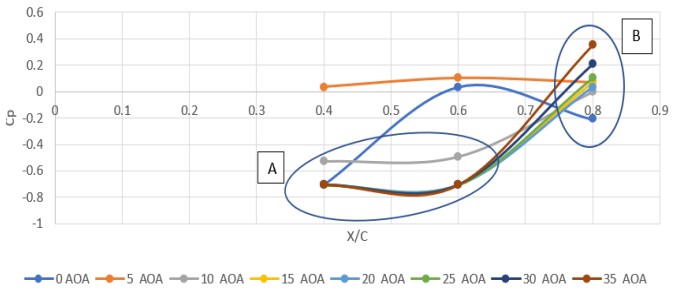

Figure 17 C_p Variation along Group 1

At Group 2 locations, shown in Figure 18, the C_p value remains positive in both regions A and B which shows the presence of vortex in the regions, but the slope is negative. So, the vortex strength is decreasing with increasing X/C except for 0° and 5° angle of attack for which the slope is positive and vortex strength is increasing from the front to the rear end of the wing

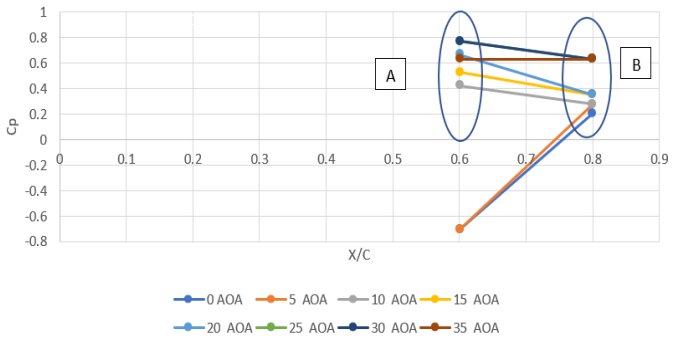

Figure 18 C_p Variation along the Group 2

3.1.4 Force testing or L/D Analysis for all leading edge shapes

Using 6 balance components on the wind tunnel the lift and drag forcses are recorded for each type of leading edge and the useful information is extracted in the form of L/D.

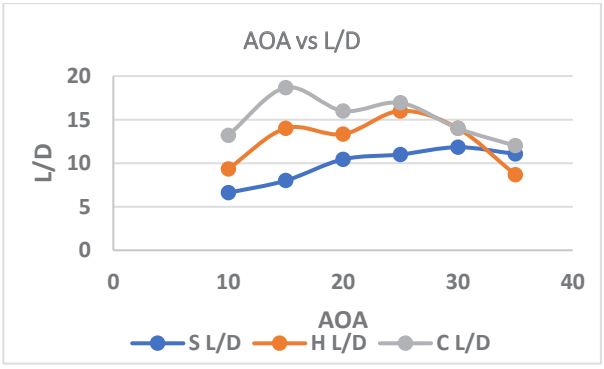

Figure 19 Variation of L/D in three different Delta Wings at various AOA's

From the data obtained above the L/D ratio represents the Aerodynamic efficiency of the wing. L/D is in the ascending order: Sharp < Hybrid < Circular.

4 CONCLUSIONS

In conclusion, the results show an advantage of increasing the leading edge radius. Vortex generation and suction lift can be seen in all the leading edge shapes. The vortex is sustained along the chord line by the circular leading edge and the flow separation is also least in this case. Upon analysis of the L/D ratio for all leading edges, the L/D of Circular LE is highest for most AOAs except for 35^0 AOA.

It can be inferred that a larger Radius of the leading edge i.e., a circular leading edge delays the vortex's bursting on the wing's surface.

REFERENCES

1. A. Garni, A.Z. Saeed, A. Garni, Experimental and numerical investigation of 65-degree delta and 65/40 degree double-delta wings. J. Aircr. **45**, 71–76 (2008). https://doi.org/10.2514/1.20243
2. D.C. Viola, D. Basawaraj, Numerical Simulation of 650 Delta Wing and 650/400 Double Delta Wing to Study the Behaviour of Primary Vortices on Aerodynamic Characteristics. Int. J. Eng. Res. **4** (2015). https://doi.org/10.17577/IJERTV4IS060764
3. J. Kegelman, F. Roos, Effects of leading-edge shape and vortex burst on the flowfield of a 70-degree-sweep delta-wing, in *Proceedings of the 27th Aerospace Sciences Meeting*, American Institute of Aeronautics and Astronautics, Reston, Virginia (1989). https://doi.org/10.2514/6.1989-86
4. J. Luckring, Reynolds number and leading-edge bluntness effects on a 65-deg delta wing, in *Proceedings of the 40th AIAA Aerospace Sciences Meeting & Exhibit*, American Institute of Aeronautics and Astronautics, Reston, Virigina (2002). https://doi.org/10.2514/6.2002-419
5. J.M. Luckring, Experimental Investigation Of The Flow About A 65 Delta Wing In The Nasa Langley National Transonic Facility. (Citeseer)
6. J.F. Marchman, Aerodynamics of Inverted Leading-Edge Flaps on Delta Wing. J. Aircr. **18**, 1051–1056 (1981). https://doi.org/10.2514/3.57599
7. J.J. Miau, K.T. Kuo, W.H. Liu, S.J. Hsieh, S.J. Chou, C.K. Lin, Flow developments above 50-deg sweep delta wings with different leading-edge profiles. J. Aircr. **32**, 787–794 (1995). https://doi.org/10.2514/3.46792
8. M.A. Mohamed, I. Afgan, M.H. Salim, I.K. Mohamed, Low speed aerodynamic characteristics of non-slender delta wing at low angles of attack. Alex. Eng. J. **61**, 9427–9435 (2022). https://doi.org/10.1016/j.aej.2022.03.003
9. R.E. Muir, A. Galeana, I.M. Viola, The leading-edge vortex of swift wing-shaped delta wings. R. Soc. Open Sci. **4** (2017). https://doi.org/10.1098/rsos.170077
10. A.A. Pashilkar, Surface pressure model for simple delta wings at high angles of attack. Sadhana **26**, 495–515 (2001)
11. M. Ramakrishna, C.S. Kumar, B. Venkatesh, Influence of leading edge shapes on vortex behaviour of delta wing. J. Phys. Conf. Ser. **1276** (2019). https://doi.org/10.1088/1742-6596/1276/1/012008
12. N. Verhaagen, Effects of Leading-Edge Radius on Aerodynamic Characteristics of 50o Delta Wings, in *Proceedings of the 48th AIAA Aerospace Sciences Meeting Including the New Horizons Forum and Aerospace Exposition*, American Institute of Aeronautics and Astronautics, Reston, Virigina (2010). https://doi.org/10.2514/6.2010-323
13. H. Ashley, T. Vaneck, M.A.M. Jarrah, J. Katz, Unsteady aerodynamic loading of delta wings for low and high angles of attack, in *Proceedings of the International Symposium on Nonsteady Fluid Dynamics* (1990)
14. R. Atta, D. Rockwell, Leading-edge vortices due to low Reynolds number flow past a pitching delta wing. AIAA J. **28**, 995–1004 (1990). https://doi.org/10.2514/3.25156

15. J. Bell, A. Burner, Data fusion in wind tunnel testing - Combined pressure paint and model deformation measurement, in *Proceedings of the 20th AIAA Advanced Measurement and Ground Testing Technology Conference*, American Institute of Aeronautics and Astronautics, Reston, Virginia (1988). https://doi.org/10.2514/6.1998-2500
16. C.E. Brown, W.H. Michael, Effect of Leading-Edge Separation on the Lift of a Delta Wing. J. Aeronaut. Sci. **21**, 690–694 (1954). https://doi.org/10.2514/8.3180
17. A. Çelik, M.M. Yavuz, Effect of Edge Modifications on Flow Structure of Low Swept Delta Wing. AIAA J. **54**, 1789–1797 (2016). https://doi.org/10.2514/1.J054587
18. H. Chen, C. Pan, J. Wang, Effects of the sinusoidal leading edge on delta wing performance and mechanism. Sci. China Technol. Sci. **56**, 772–779 (2013). https://doi.org/10.1007/s11431-013-5143-3
19. K. Chiba, S. Obayashi, K. Nakahashi, CFD Visualization of Second Primary Vortex Structure on a 65-Degree Delta Wing, in *Proceedings of the 42nd AIAA Aerospace Sciences Meeting and Exhibit*, American Institute of Aeronautics and Astronautics, Reston, Virigina (2024). https://doi.org/10.2514/6.2004-1231
20. C. Chivey, Navier-Stokes calculation of transonic flow past the NTF 65 deg delta wing. (Old Dominion Univ., NASA/American Society for Engineering Ed., 1991)
21. J. Chu, J.L. Luckring, Experimental Surface Pressure Data Obtained on 65 ̊delta Wing Across Reynolds Number and Mach Number Ranges. (National Aeronautics and Space Administration, Langley Research Center, **1**, 1966)
22. E.C. Polhamus, Predictions of vortex lift characteristics by a leading edge suction analogy. J. Aircr. **8**, 193-9 (1971)